

RNA N6-methyladenosine methyltransferase WTAP promotes the differentiation of endothelial progenitor cells

LONGYUN WU^{1*}, LILI NIU^{1-3*}, ZHOU YANG^{1,4*}, QIAOYUN XIA¹, JINGYUAN XU^{1,5} and XIAOLAN LU^{1,5}

¹Department of Gastroenterology, Fudan University Pudong Medical Center, Shanghai 201399;

²Central Laboratory, First Affiliated Hospital of Dalian Medical University; ³Institute of

Integrative Medicine, Dalian Medical University, Dalian, Liaoning 116021; ⁴Department of

Cardiovascular Surgery, Fudan University Shanghai Cancer Center, Shanghai 200120; ⁵Department of

Gastroenterology, The Second Affiliated Hospital of Xi'an Jiaotong University, Xi'an, Shaanxi 710004, P.R. China

Received February 5, 2023; Accepted June 23, 2023

DOI: 10.3892/etm.2023.12119

Abstract. N6-methyladenosine (m⁶A) serves a critical role in regulating gene expression and has been associated with various diseases; however, its role in the differentiation of endothelial progenitor cells (EPCs) remains unclear. The present study used liquid chromatography with tandem mass spectrometry and immunofluorescence assays to quantify the levels of m⁶A in human peripheral blood-derived EPCs (HPB-EPCs) before and after differentiation into mature cells. The present study performed Cell Counting Kit 8, Transwell, and tube formation assays to determine the effects of overexpression and knockdown of Wilms' tumor 1-associated protein (WTAP) on HPB-EPCs. The results revealed that the level of m⁶A modification was significantly increased during HPB-EPCs differentiation, and WTAP exhibited the most significant alteration among the enzymes involved in m⁶A regulation. When WTAP was overexpressed in HPB-EPCs, cell proliferation, invasion, and the formation of tubes were improved, whereas WTAP knockdown yielded the opposite effects. In conclusion, the present study highlighted the involvement of m⁶A in regulating EPC differentiation, with WTAP acting as a promoter of EPC differentiation.

Introduction

Endothelial progenitor cells (EPCs) are the precursors of vascular endothelial cells (1), which can be mobilized from

the bone marrow to peripheral blood in response to physiological or pathological conditions for endothelial repair and neovascularization (2,3). EPC-induced vasculogenesis has been considered to provide a novel therapeutic approach for patients with heart and limb ischemia. Various approaches have been explored to enhance EPC grafting, including local EPC delivery, promotion of EPC mobilization, EPC function enhancement, and *in vitro* EPC expansion (4). However, the biology of EPCs is complex and understanding of the precise mechanisms that regulate EPC differentiation is limited (5).

N6-methyladenosine (m⁶A) is the most common internal modification in eukaryotic RNA (6,7). It can regulate multiple physiological processes, including stem cell differentiation, animal growth and development, *Drosophila* sex determination and DNA damage repair (8). The effectors of m⁶A include 'writers' and 'erasers', which install and remove the methyl group, respectively, and 'readers', which recognize methylation (9-12). The core writer complex, consisting of methyltransferase-like (METTL)3 and METTL14, forms a stable heterodimer complex that catalyzes m⁶A modification (9). It has been established that Wilms' tumor 1-associated protein (WTAP) binds to this heterodimer complex and facilitates its nuclear localization, thus promoting the deposition of m⁶A (13). Accordingly, the m⁶A levels are largely dependent on this methyltransferase complex. Moreover, it is now understood that WTAP is involved in several biological functions, including embryo development, cell cycle progression, cell differentiation, pre-mRNA splicing, and antiviral responses (14-16).

Notably, m⁶A has been studied in stem cell differentiation. Previous studies have documented the effect of enzymes associated with m⁶A regulation on stem cells. In this respect, it has been reported that YTHDF2 is essential for self-renewing hematopoietic stem cells (17). Notably, Chen *et al* (18) revealed that doxycycline-induced fusion of dCas13a with the catalytic domain of ALKBH5 could demethylate m⁶A-enriched SOX2 and control the differentiation of human embryonic stem cells. Moreover, elevated levels of m⁶A have been documented in cancer stem cells (CSCs) (19,20). Although it has been established that m⁶A can promote the expression of oncogenes in CSCs (19), it can also promote the tumor phenotype of CSCs

Correspondence to: Dr Jingyuan Xu or Professor Xiaolan Lu, Department of Gastroenterology, Fudan University Pudong Medical Center, 2800 Gongwei Road, Shanghai 201399, P.R. China
E-mail: 498520087@qq.com
E-mail: xiaolan_lu@163.com

*Contributed equally

Key words: N6-methyladenosine, endothelial progenitor cell, cell differentiation, Wilms' tumor 1-associated protein

and metastasis (21). While previous studies have primarily focused on m⁶A in the context of CSCs, investigations into m⁶A in EPCs have been relatively scarce (22). The present study focused on the m⁶A ‘writer’ WTAP in EPC differentiation. The study aimed to investigate the dynamics of m⁶A levels during the differentiation process of HPB-EPCs and identify the key enzyme involved in regulating m⁶A that impacted this process. These findings may illuminate an effective mechanism for promoting vascular repair through m⁶A.

Materials and methods

Isolation of HPB-EPCs, overexpression, and knockdown of WTAP. The present study was approved by the Medical Ethics Committee of Fudan University Pudong Medical Center (Shanghai, China; approval no. 2020-SZR-04) and written informed consent was obtained from the participants. Venous blood samples (15 ml) from three healthy male donors aged 25–28 years were aseptically collected in the blood collection room at the hospital's experimental center by a trained nurse. Then the peripheral blood was diluted with PBS before being added to human lymphocyte separation medium (cat. no. P8610; Beijing Solarbio Science and Technology, Co., Ltd.). After centrifugation at 500 × g for 20 min at room temperature, the mononuclear cell layer was isolated and washed twice with an equal volume of PBS containing 2% fetal bovine serum (FBS; Gibco; Thermo Fisher Scientific, Inc.). The differentiation of EPCs was induced using complete endothelial cell medium (ECM; cat. no. 1001; ScienCell Research Laboratories, Inc.) containing 5% FBS, 5% endothelial cell growth supplement (cat. no. 1052; ScienCell Research Laboratories, Inc.), 100 U/ml penicillin and 100 µg/ml streptomycin (cat. no. 0503; ScienCell Research Laboratories, Inc.). The cells were cultured in an incubator containing 5% CO₂ at 37°C, and cell growth was monitored every other day using an inverted light microscope. The first day of induction *in vitro* (1D) marks the initiation, while the fourteenth day of induction (14D) refers to a specific time point during the process.

To induce overexpression of WTAP, the coding sequence of WTAP was inserted into the pLVX-Puro plasmid (cat. no. HH-LV-048; HedgehogBio Science and Technology, Ltd.). For WTAP knockdown, WTAP-specific short hairpin (sh)RNA #1–3 and the scrambled (scr) sequence that was used as a negative control (NC), were ligated to the linearized pLKO.1-Puro plasmid (cat. no. HH-shRNA-004; HedgehogBio Science and Technology, Ltd.). The study utilized a second-generation lentiviral packaging system comprising of three plasmids to conduct the experiments. Table I provides a comprehensive overview of the sequence information for shRNA #1–3 and Scr (NC). The 5 µg recombinant plasmids, along with the psPAX2 packaging plasmid and pMD2G envelope plasmid at a ratio of 4:3:1, were transfected into 293T cells (cat. no. FH0244; Fuheng Biotechnology, Ltd.) using Lipofectamine™ 3000 (cat. no. L3000015; Invitrogen; Thermo Fisher Scientific, Inc.). A total of 48 h post-transfection, the supernatant was collected and filtered to obtain the virus for subsequent transduction. For overexpression of WTAP, a blank vector was used as an NC. Well-cultured HPB-EPCs at a confluence of 40% were pre-selected and the aforementioned viral particles were added to the supernatant of HPB-EPCs at

an MOI of 200. After being cultured for 24 h in an incubator set at 37°C, the virus-containing culture medium was replaced with fresh culture medium. A total of 3 days post-transduction, fluorescence expression in cells was observed and stable cell lines were screened using 5 µg/ml puromycin for 24 h prior to subsequent experiments, while a maintenance dose of 2 µg/ml puromycin was used during the experiment.

Cell proliferation assay. Exponential phase HPB-EPCs were resuspended with complete ECM following digestion with trypsin. The cells were counted and seeded into a 96-well plate at a density of 2,000 cells/well. After incubation for 0, 24, 48, and 72 h, the culture medium containing 10% Cell Counting Kit 8 (CCK8; Dojindo Laboratories, Inc.) was added to the cells and incubated for 2 h within the CO₂ incubator, all at 37°C. Subsequently, the absorbance of the samples was measured at a wavelength of 450 nm using a spectrophotometer.

Cell invasion assay. The cell invasion assay was performed using Transwell plates (24-well insert; pore size, 8 µm; BD Biosciences). The filter membrane of the chamber was coated with 60 µl Matrigel (1:8 dilution; BD Biosciences) for 1 h at 37°C. The upper chamber was seeded with 100 µl serum-free medium containing 2 × 10⁴ HPB-EPCs and the lower chamber was seeded with 600 µl complete ECM. After incubation for 24 h at 37°C, the chamber was fixed with 4% paraformaldehyde for 30 min and stained with 0.1% crystal violet for 30 min at room temperature. Finally, a magnifying light microscope (Leica DMI3000B; Leica Microsystems GmbH) was used to count the number of invaded cells at the bottom of the chamber.

Tube formation assay. Precooled 96-well plates were seeded with 100 µl/well Matrigel (BD Biosciences) and incubated at 37°C for 30 min. Subsequently, the stably transfected cells were trypsinized, resuspended in complete ECM, seeded at 5 × 10⁴/well in the aforementioned 96-well plates, and incubated for another 6 h at 37°C. Finally, images were captured using the white light channel of a fluorescence microscope (Nikon Corporation). The number and length of tubes were counted and analyzed by ImageJ (version 1.8.0; National Institutes of Health).

Liquid chromatography with tandem mass spectrometry (LC-MS/MS) assay. TRIzol® Reagent (cat. no. 15596026; Invitrogen; Thermo Fisher Scientific, Inc.) was employed to isolate total RNA from HPB-EPCs on 1D and 14D. Oligo dT magnetic beads (cat. no. 19820; Yeasen Biotechnology, Ltd.) were used to purify mRNA from total RNA. Subsequently, 200 ng purified mRNA was incubated with nuclease P1 (0.5 U; MilliporeSigma) at 42°C for 1 h in a reaction system containing 10 mM NH₄OAc (pH, 5.3; 25 µl). Then, NH₄HCO₃ (1 M; 3 µl) and alkaline phosphatase (1 µl; 1 U/µl; MilliporeSigma) were added and incubated at 37°C for 2 h. After neutralization with 1 µl HCl (3 M), samples were diluted to 50 µl and filtered through a 0.22-µm filter (MilliporeSigma). The separation of all samples (10 µl per injection) was achieved using reverse-phase ultra-performance LC through an ACQUITY UPLC T3 column (Waters Technologies, Inc.). The flow rate was 0.3 ml/min. Analysis was performed using a TripleTOF

Table I. shRNA and primer sequences used in the present study.

shRNA or primer	Sequence, 5'-3'
Human WTAP shRNA #1	GGUUCGAUUGAGUGAAACATT
Human WTAP shRNA #2	GCUUUGGAGGGCAAGUACATT
Human WTAP shRNA #3	GGGCAACACAACCGAAGAT
Scr (NC)	CAACAAGATGAAGAGCACCAAC
CD133	F: AGTCGGAAACTGGCAGATAGC R: GGTAGTGTGTACTGGGCCAAT
KDR	F: GGCCCAATAATCAGAGTGGCA R: CCAGTGTCAATTTCCGATCACTTT
vwF	F: CCGATGCAGCCTTTTCGGA R: TCCCCAAGATACACGGAGAGG
CD31	F: AACAGTGTGACATGAAGAGCC R: TGTA AAAACAGCACGTCATCCTT
METTL3	F: TCTCCACGCCAGATGCTC R: ACAGTCCCTGCTACCTCCC
METTL14	F: CCTCCATGTACTTACAAGCC R: TAGCAGTGATGCCAGTTTCTC
WTAP	F: ATGGCGAAGTGTCCAATGC R: CCAACTGCTGGCGTGTCTC
FTO	F: ACTTGGCTCCCTTATCTGACC R: TGTGCAGTGTGAGAAAGGCTT
ALKBH5	F: CGGCGAAGGCTACACTTACG R: CCACCAGCTTTTGGATCACCA
IGF2BP1	F: TCCCCGATGAGCAGATAGC R: CTGGGTCTGTTTTGTGATGTTG
IGF2BP2	F: ATGAAACAGGGACCAAGATAAC R: GTTGAAAAGATGCCAAGTGC
IGF2BP3	F: GATTAAATCTGAACGCCTTGG R: TGGCACCGACTGATAGAGC
YTHDF1	F: ACCTGTCCAGCTATTACCCG R: TGGTGAGGTATGGAATCGGAG
YTHDF2	F: AGCCCACTTCTACCAGATG R: TGAGA ACTGTTATTTCCCATGC
YTHDF3	F: TCAGAGTAACAGCTATCCACCA R: GGTGTGCAGATATGGCATAGGCT
GAPDH	F: GGAGCGAGATCCCTCCAAAAT R: GGCTGTTGTCATACTTCTCATGG

F, forward; NC, negative control; scr, scrambled; shRNA, short hairpin RNA; R, reverse.

6600 tandem mass spectrometer (SCIEX Technologies, Inc.) in positive electrospray ionization mode. The interface heater temperature was 550°C. The curtain gas was set at 30 PSI, and both Ion source gas1 and Ion source gas2 were all set at 55 PSI. All nucleosides were quantified using retention times, and ion mass transitions (m/z) from 268.1 to 136.1 [Adenosine (A)] and 282.1 to 150.1 (m⁶A). Quantification was performed using standard curves generated within the same experimental

batch. A calibration curve was derived from these standard curves to calculate the m⁶A to A ratios (23).

Immunofluorescence. The cells were fixed with 4% paraformaldehyde for 20 min at room temperature and were then incubated with 0.3% Triton X-100 for 10 min, and the non-specific binding sites were blocked with 5% BSA (cat. no. SW3015; Beijing Solarbio Science and Technology, Co., Ltd.) for 30 min at room temperature. Subsequently, the cells were incubated with a primary antibody against m⁶A (cat. no. A-1801; EpiGentek, Inc.) at a dilution of 1:100 overnight at 4°C, followed by a 1:1,000 dilution of Alexa Fluor[®] 594-conjugated goat anti-rabbit secondary antibody (cat. no. 8889; Cell Signaling Technology, Inc.) at room temperature for 1 h. Finally, nuclear staining was performed with DAPI for 1 min at room temperature, and cells were observed with EVOS[™] FL Auto 2 imaging system (Invitrogen; Thermo Fisher Scientific, Inc.).

Western blotting. Protein samples were extracted from the experimental cells using protein lysis buffer, which contained RIPA lysis buffer (cat. no. PC101; Epizyme Biomedical Technology, Ltd.) and 1X protease inhibitor cocktail (cat. no. GRF101; Epizyme Biomedical Technology, Ltd.). The extracted proteins were then quantified using the BCA method, denatured using sample buffer, separated by 10% SDS-PAGE with loading of 20 µg protein per well and electrophoretically transferred to PVDF membranes. The membranes were then exposed to a blocking solution (cat. no. PS108P; Epizyme Biomedical Technology, Ltd.) for 10 min at room temperature and incubated overnight with the primary antibodies at 4°C. The membranes were then washed three times with TBST (containing 0.1% Tween20) and incubated with an HRP-conjugated secondary antibody for 1 h at room temperature. Signals were detected and captured using a filesystem (GBOX; Syngene) with a luminescence solution (cat. no. SQ201L; Epizyme Biomedical Technology, Ltd.) (liquids A and B; 1:1 ratio). The primary antibodies utilized in this investigation were WTAP (cat. no. 41934; Cell Signaling Technology, Inc.) and β-actin (cat. no. 4970; Cell Signaling Technology, Inc.), both at a dilution of 1:1,000. The secondary antibody employed was HRP-linked anti-rabbit antibody (cat. no. 7074; Cell Signaling Technology, Inc.) at a dilution of 1:3,000.

Reverse transcription-quantitative PCR (RT-qPCR). RNA samples were extracted from cells using TRIzol[®] Regent (cat. no. 15596026; Invitrogen; Thermo Fisher Scientific, Inc.) and reverse transcribed (cat. no. RR037A; Takara Bio, Inc.) according to the manufacturer's instructions. cDNA was diluted in nuclease-free water and RT-qPCR was performed using 50 ng diluted cDNA, the TB Green[®] Premix Ex Taq[™] kit (cat. no. RR420A; Takara Bio, Inc.), and the ABI 7500 Real-Time PCR system (Applied Biosystem; Thermo Fisher Scientific, Inc.) according to the manufacturer's instructions. The thermocycling protocol was established based on the manufacturer's instructions and the specifications of the RT-PCR instrument utilized, as follows: Denaturation for 1 cycle at 95°C for 30 sec, followed by PCR for 40 cycles at 95°C for 5 sec and 60°C for 34 sec, and then melting

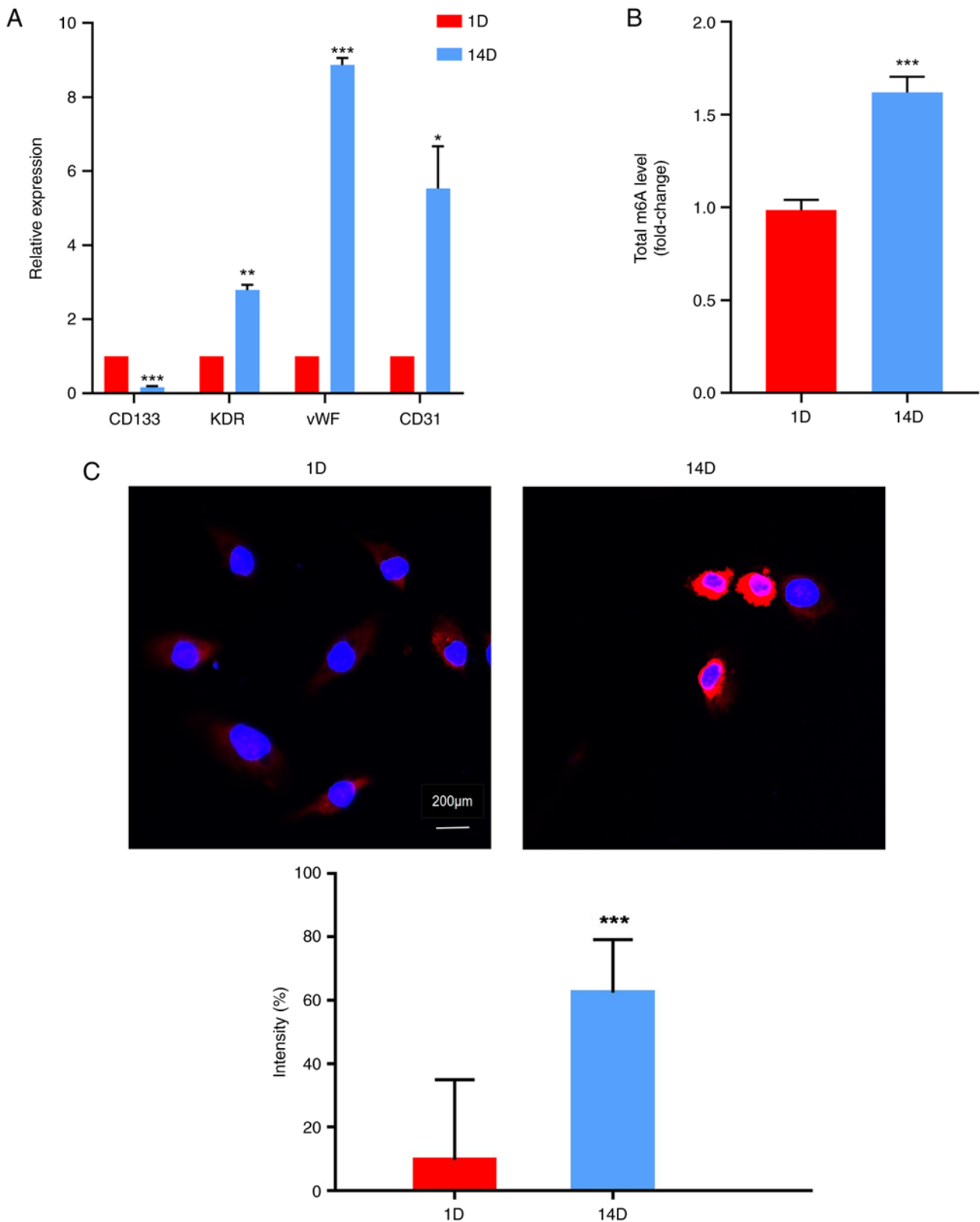


Figure 1. M⁶A levels are increased with the differentiation of EPCs. (A) Relative expression levels of cell surface markers of human peripheral blood-derived EPCs at different time points (1D and 14D) were detected by quantitative PCR. Expression levels of cell lineage marker CD133 and reendothelialization markers KDR, vWF, and CD31 were assessed at different time points during EPC culture. CD133 expression decreased over time, whereas KDR, vWF and CD31 expression increased. m⁶A levels were quantified in differentiated EPCs by (B) LC-MS/MS and (C) immunofluorescence assays. Differentiated EPCs exhibited higher m⁶A levels. *P<0.05, **P<0.01, ***P<0.001 vs. 1D. D, day; EPC, endothelial progenitor cell; m⁶A, N⁶-methyladenosine; vWF, von Willebrand factor.

for 1 cycle at 95°C for 15 sec, 60°C for 1 min and 95°C for 15 sec. GAPDH was employed as the housekeeping gene in

this experiment. All primers used in the present study were sourced from Thermo Fisher Scientific, Inc., and are listed

in Table I. The final results were analyzed using the $2^{-\Delta\Delta Cq}$ method (17).

Statistical analysis. Statistical analysis was conducted using Prism 9 software (GraphPad; Dotmatics). Data are presented as the mean \pm standard error of the mean. The significance level (α) was set at 0.05. $P < 0.05$ was used to indicate a statistically significant difference. Comparisons between two groups were evaluated using unpaired two-tailed Student's t-test for data exhibiting normal distribution based on the Shapiro-Wilk normality test. For multiple comparisons, one-way ANOVA and LSD post hoc test was performed. Immunofluorescence, western blotting, and qPCR were performed with at least three independent biological replicates. The sample size was not predetermined using a statistical method, but a minimum of three samples were included in each experimental group and condition.

Results

M⁶A levels are increased with the differentiation of EPCs. It has been established that the differentiation of EPCs can be identified by detecting specific cell markers (24,25). To evaluate the differentiation of HPB-EPCs, the expression levels of cell surface markers were detected at different time points (1D and 14D) using RT-qPCR. The expression levels of the cell lineage marker CD133 were significantly downregulated with increased culture duration (Fig. 1A). By contrast, markers associated with endothelialization, including KDR, von Willebrand factor (vWF), and CD31, were significantly upregulated on 14D compared with on 1D (Fig. 1A). These findings suggested that EPCs could differentiate into endothelial cells during prolonged culture *in vitro*. Furthermore, m⁶A modification levels were investigated at different time points during EPC culture using LC-MS/MS and immunofluorescence techniques. Table SI provides information regarding the raw and normalized peaks detected by LC-MS/MS. The results revealed that the differentiated EPCs exhibited higher levels of m⁶A modification than undifferentiated cells (Fig. 1B and C).

WTAP contributes to increased m⁶A levels in EPCs. The mRNA expression levels of multiple m⁶A-related enzymes were detected during EPCs differentiation by RT-qPCR. Compared with pre-differentiation EPCs, the mRNA expression levels of a variety of methyltransferases ('writers', such as METTL14 and WTAP), demethylases ('erasers', such as FTO and ALKBH5), and methylation-recognition enzymes ('readers', for example, IGF2BP1-3 and YTHDF1-2) were significantly increased (except for METTL3 and YTHDF3) after differentiation (Fig. 2A), suggesting that m⁶A was increased after HPB-EPCs differentiation. Among all enzymes, the mRNA expression levels of WTAP were increased the most after the differentiation of HPB-EPCs. Western blotting further verified that the protein expression levels of WTAP were significantly increased after differentiation (Fig. 2B), suggesting that WTAP may play a major role in EPCs differentiation. To investigate the effect of WTAP on EPCs differentiation, overexpression and knockdown of WTAP were successfully induced in HPB-EPCs and were verified using western blotting. Compared to the control group, the overexpression group

exhibited an increase in WTAP protein expression. While EPC-shWTAP-1 did not markedly alter the expression level, the EPC-shWTAP-2 and EPC-shWTAP-3 groups, which were selected for subsequent experiments, exhibited a significant reduction in protein expression compared with the negative control group (EPC-scr; Fig. 2C). Subsequently, an immunofluorescence assay was employed to detect alterations in m⁶A levels resulting from overexpression and knockdown of WTAP in HPB-EPCs. Overexpression of WTAP in HPB-EPCs led to an increase in m⁶A level, whereas knockdown of WTAP resulted in a downregulation of m⁶A level (Fig. 2D). These findings suggested that WTAP may have a crucial role in regulating m⁶A during EPC differentiation. Subsequently, the present study evaluated the effects of changes in WTAP expression on EPC proliferation, invasion, and tube formation.

Overexpression of WTAP promotes the differentiation of EPCs. Compared with the EPC-NC group, the proliferation of EPCs was increased after WTAP overexpression in a time-dependent manner and was significant after 72 h of culture (Fig. 3A). During the Transwell assay, HPB-EPCs with WTAP overexpression exhibited a higher number of cells crossing the filter membrane compared with that in the EPC-NC group, suggesting that the overexpression of WTAP enhanced the invasive ability of the cells (Fig. 3B). In addition, the EPC-WTAP group showed increased formation of tubes and branching, suggesting that EPCs overexpressing WTAP exhibited enhanced tube formation ability (Fig. 3C).

Knockdown of WTAP inhibits the differentiation of EPCs. The present study demonstrated that the EPC-WTAP group exhibited increased proliferation, invasion, and tube formation. Subsequently, the present study explored the effects of knocking down WTAP on the aforementioned functions in EPCs. The CCK8 assay revealed that the proliferation of EPCs was decreased by WTAP knockdown compared with in the NC group after 72 h of culture (Fig. 4A). In contrast to the EPC-scr group, cell invasion and tube formation were decreased following WTAP knockdown (Fig. 4B and C).

Discussion

Current evidence (26,27) suggests that EPCs have similar differentiation capabilities to stem cells, and their surface markers undergo changes at different stages during the differentiation process. During the differentiation of EPCs, CD133 expression is gradually downregulated on the cell surface, whereas the immunophenotype of differentiated EPCs is characterized by the presence of CD31, VE-cadherin, vWF, CD146 and VEGFR2/KDR, and the lack of CD45 and CD14 expression (24,25). The present study revealed that EPCs exhibited differentiation ability *in vitro*. Notably, the levels of m⁶A were increased with the differentiation of EPCs; however, the role of m⁶A in EPC differentiation remains unclear, warranting further exploration.

Little is currently known about the role of m⁶A in stem cell regulation, since most studies have focused on the role of m⁶A in CSCs (18-21,28). It has been established that the levels of m⁶A are upregulated in CSCs, and that the key enzymes involved in m⁶A regulation may influence the phenotype of CSCs, promote

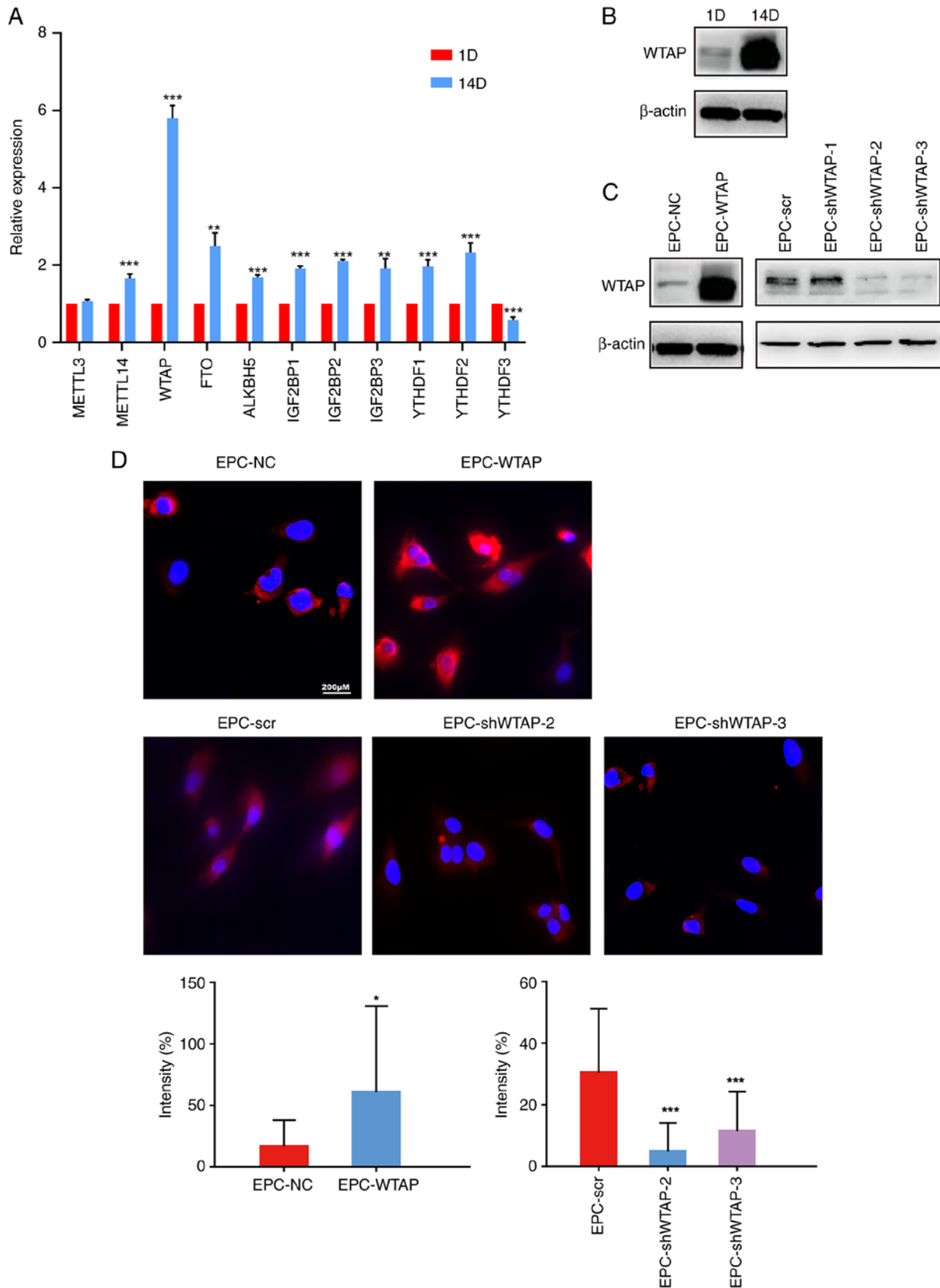


Figure 2. WTAP contributes to increased m⁶A levels in EPCs. (A) mRNA expression levels of m⁶A-related enzymes during EPC differentiation, as detected by quantitative PCR. After differentiation, the expression levels of METTL14, WTAP, FTO, ALKBH5, IGF2BP1-3 and YTHDF1-2 were significantly higher than in EPCs before differentiation. **P<0.01, ***P<0.001 vs. 1D. (B) Western blotting was used to verify the protein expression levels of WTAP, which were also increased after cell differentiation. (C) WTAP expression was validated by western blot analysis following overexpression and knockdown of WTAP. Compared with the control group, the overexpression group exhibited an increase in WTAP protein expression, whereas the knockdown group showed a decrease in WTAP protein expression (with the exception of EPC-shWTAP-1). (D) Immunofluorescence assays were performed to validate alterations in m⁶A following the successful overexpression and knockdown of WTAP in HPB-EPCs. Overexpression of WTAP in HPB-EPCs increased m⁶A levels, whereas knockdown of WTAP resulted in a decrease in m⁶A levels. *P<0.05 vs. EPC-NC; ***P<0.001 vs. EPC-scr. D, day; EPC, endothelial progenitor cell; m⁶A, N⁶-methyladenosine; NC, negative control; scr, scrambled; sh, short hairpin; WTAP, Wilms' tumor 1-associated protein.

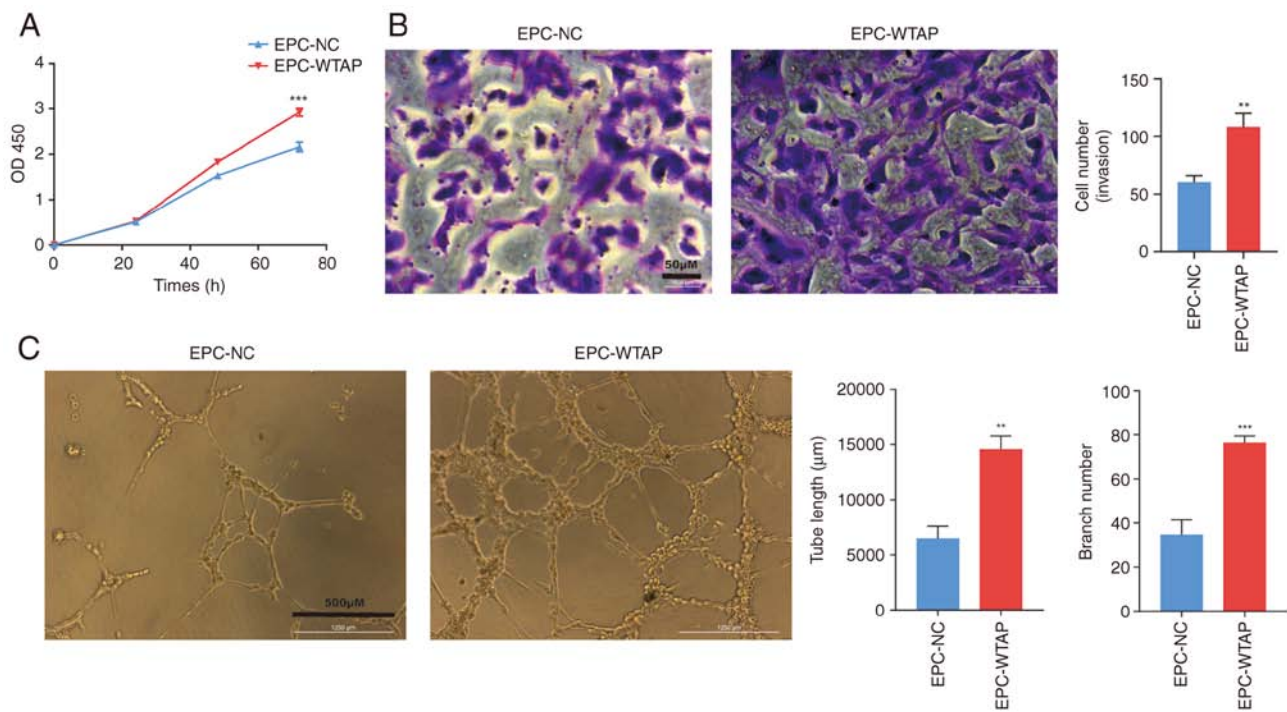


Figure 3. Overexpression of WTAP promotes the differentiation of EPCs. (A) Proliferation of EPC-NC and EPC-WTAP at different times, as determined by Cell Counting Kit 8. In contrast to EPC-NC, the proliferation of EPCs increased after WTAP overexpression in a time-dependent manner and was significant after 72 h of culture. (B) Invasion of EPCs overexpressing WTAP was demonstrated through a Transwell assay; more cells overexpressing WTAP crossed the filter membrane. (C) Tube formation assay was performed to evaluate the tube-forming ability of EPCs. EPC-WTAP formed more tubes and more branches. ** $P < 0.01$, *** $P < 0.001$ vs. EPC-NC. EPC, endothelial progenitor cell; NC, negative control; WTAP, Wilms' tumor 1-associated protein.

tumor metastasis, and influence tumor prognosis (18-21,28). m^6A can affect endothelial function and vascular permeability, and can participate in the regulation of atherosclerosis. Endothelial inflammation has been shown to be made worse by METTL14 (29), and oxidative low-density lipoprotein can make human umbilical vein endothelial cells less likely to divide and move (11). A previous study revealed that CPEB2 in glioma microvascular endothelial cells enhances SRSF5 stability and promotes the expression of ZO-1, occludin, and claudin-5 to protect vascular integrity through m^6A modification (upregulation of METTL3 and methylation-recognition enzyme IGF2BP3) (30). However, studies investigating the role of m^6A in EPCs are limited. A previous study has revealed that knockdown of METTL3 in EPCs could result in impaired angiogenic potential; by contrast, overexpression of METTL3 in EPCs led to enhanced tube formation with increased tubule branching and increased angiogenesis in the chorioallantoic membrane of chicken embryos (22). Similarly, the present study showed that WTAP, another m^6A methyl transferase, enhanced the tubulogenic capacity of EPCs *in vitro*.

It is well known that METTL3, METTL14, and WTAP form the m^6A methyl transferase complex (MTC) (12). WTAP, an essential regulatory subunit in methyltransferases, recruits the MTC to the target mRNA (31). Current evidence suggests that WTAP has various biological functions, including embryonic development, cell cycle progression and differentiation, precursor mRNA splicing, and alternative splicing (12). WTAP is also crucial in several pathological processes, such as worsening myocardial ischemia-reperfusion injury by increasing endoplasmic reticulum stress (32), inducing malignant tumor growth (12), and possibly increasing resistance of tumors to

drugs (33). The present study demonstrated that WTAP could promote the proliferation, invasion, and angiogenesis of EPCs, suggesting that WTAP may promote the differentiation of EPCs.

The present study observed that the expression trend of YTHDF3 differed from that of other m^6A enzymes in response to EPC differentiation. The other enzymes involved in m^6A modification showed an increasing trend during EPC differentiation, whereas YTHDF3 showed a decreasing trend. The exact role of YTHDF proteins in pluripotent stem cells remains uncertain. After conducting phenotypic and transcriptomic analysis, Wang *et al* (34) discovered that the absence of YTHDF1 in embryonic stem cells can result in a significant hindrance to cardiomyocyte (CM) differentiation, whereas YTHDF3 knockdown can facilitate CM-specific gene expression and thus promote CM differentiation. Based on these findings, it was hypothesized that YTHDF3 may exhibit a downward trend during EPCs differentiation. However, there is limited research on the role of YTHDF3 in EPCs differentiation and further investigations are needed to provide conclusive evidence supporting this hypothesis.

To the best of our knowledge, the present study is the first to provide evidence of the involvement of the m^6A methyltransferase WTAP in regulating EPC differentiation; however, there are limitations. First, the present study only included *in vitro* experiments, and future *in vivo* vascular experiments are warranted to further evaluate the effect of WTAP on the differentiation of EPCs. Second, due to study limitations, RT-qPCR was used instead of flow cytometry to detect cell surface markers and to evaluate EPCs

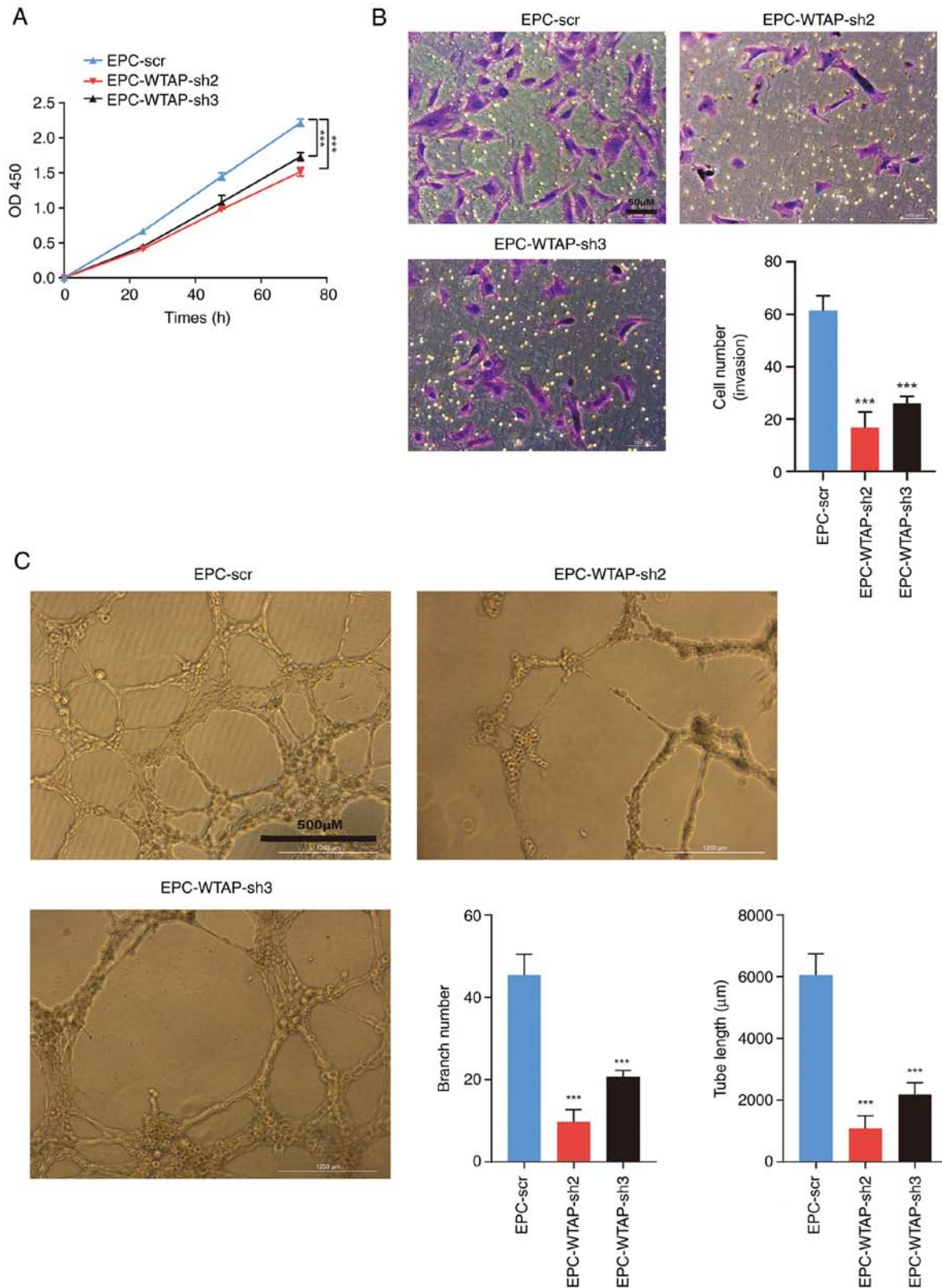


Figure 4. Knockdown of WTAP inhibits the differentiation of EPCs. (A) Cell Counting Kit 8 was used to analyze the proliferation of EPC-scr, EPC-WTAP-sh2 and EPC-WTAP-sh3 at different times. EPC proliferation was decreased after 72 h of culture following WTAP knockdown. (B) Invasion and (C) tube formation were determined using Transwell and tube formation assays, respectively. In contrast to EPC-scr, cell invasion, and tube formation were decreased after WTAP knockdown. *** $P < 0.001$ vs. EPC-scr. EPC, endothelial progenitor cell; scr, scrambled; sh, short hairpin; WTAP, Wilms' tumor 1-associated protein.

differentiation. Third, the present study primarily focused on observing the phenomenon without exploring the underlying mechanisms. To elucidate the mechanism, techniques such as gene chip analysis should be employed to identify potential

target genes and pathways involved in WTAP-mediated EPC differentiation.

In conclusion, the present study revealed that m⁶A is involved in regulating EPC differentiation, and WTAP, one of

its methyltransferases, may promote the proliferation, invasion, and tube formation of EPCs, thus indicating that WTAP may promote the differentiation of EPCs.

Acknowledgements

Not applicable.

Funding

This research is supported by the Shanghai Pudong Hospital (grant no. YJRCJJ201801), the Natural Science Foundation of Shanghai (grant no. 20ZR1450100), and the Natural Science Foundation of China (grant no. 82070587).

Availability of data and materials

The datasets used and/or analyzed during the current study are available from the corresponding author on reasonable request.

Authors' contributions

JX, ZY, LN, LW and XL conceived and designed the study. JX, LW, LN, ZY, QX and XL conducted the experiments. LN, ZY and LW analyzed the data. LW and ZY wrote the manuscript. ZY, JX and XL confirm the authenticity of all the raw data. JX and XL revised the manuscript. All authors read and approved the final manuscript.

Ethics approval and consent to participate

Since the present study involved collecting blood samples from participants, the contents of the experiment were reviewed and approved by the Medical Ethics Committee of Fudan University Pudong Medical Center, and all of the participants provided written informed consent. In the consent form, the experimental procedures were detailed, including the possibly associated risks and the benefits to the participants, and it informed them in writing that their specimens would be used only for scientific research and there would be no commercial use.

Patient consent for publication

Not applicable.

Competing interests

The authors declare that they have no competing interests.

References

- Asahara T, Murohara T, Sullivan A, Silver M, van der Zee R, Li T, Witzenbichler B, Schatteman G and Isner JM: Isolation of putative progenitor endothelial cells for angiogenesis. *Science* 275: 964-967, 1997.
- Psaltis PJ and Simari RD: Vascular wall progenitor cells in health and disease. *Circ Res* 116: 1392-1412, 2015.
- Bonder CS, Sun WY, Matthews T, Cassano C, Li X, Ramshaw HS, Pitson SM, Lopez AF, Coates PT, Proia RL, *et al*: Sphingosine kinase regulates the rate of endothelial progenitor cell differentiation. *Blood* 113: 2108-2117, 2009.
- Tasev D, Koolwijk P and van Hinsbergh VW: Therapeutic potential of human-derived endothelial colony-forming cells in animal models. *Tissue Eng Part B Rev* 22: 371-382, 2016.
- Kim J, Kim M, Jeong Y, Lee WB, Park H, Kwon JY, Kim YM, Hwang D and Kwon YG: BMP9 induces cord blood-derived endothelial progenitor cell differentiation and ischemic neovascularization via ALK1. *Arterioscler Thromb Vasc Biol* 35: 2020-2031, 2015.
- He L, Li H, Wu A, Peng Y, Shu G and Yin G: Functions of N6-methyladenosine and its role in cancer. *Mol Cancer* 18: 176, 2019.
- Boulias K and Greer EL: Biological roles of adenine methylation in RNA. *Nat Rev Genet* 24: 143-160, 2023.
- Frye M, Harada BT, Behm M and He C: RNA modifications modulate gene expression during development. *Science* 361: 1346-1349, 2018.
- Shi H, Wei J and He C: Where, when, and how: Context-Dependent functions of RNA methylation writers, readers, and erasers. *Mol Cell* 74: 640-650, 2019.
- Wang T, Kong S, Tao M and Ju S: The potential role of RNA N6-methyladenosine in cancer progression. *Mol Cancer* 19: 88, 2020.
- Rong J, Jie Y and Zhao H: m6A 'writer' KIAA1429 regulates the proliferation and migration of endothelial cells in atherosclerosis. *Mol Biotechnol* 65: 1198-1206, 2023.
- Huang Q, Mo J, Liao Z, Chen X and Zhang B: The RNA m⁶A writer WTAP in diseases: Structure, roles, and mechanisms. *Cell Death Dis* 13: 852, 2022.
- Wang LJ, Xue Y, Li H, Huo R, Yan Z, Wang J, Xu H, Wang J, Cao Y and Zhao JZ: Wilms' tumor 1-associating protein inhibits endothelial cell angiogenesis by m6A-dependent epigenetic silencing of desmoplakin in brain arteriovenous malformation. *J Cell Mol Med* 24: 4981-4991, 2020.
- Wang Z, Qi Y, Feng Y, Xu H, Wang J, Zhang L, Zhang J, Hou X, Feng G and Shang W: The N6-methyladenosine writer WTAP contributes to the induction of immune tolerance post kidney transplantation by targeting regulatory T cells. *Lab Invest* 102: 1268-1279, 2022.
- Horiuchi K, Kawamura T, Iwanari H, Ohashi R, Naito M, Kodama T and Hamakubo T: Identification of Wilms' tumor 1-associating protein complex and its role in alternative splicing and the cell cycle. *J Biol Chem* 288: 33292-33302, 2013.
- Sacco MT, Bland KM and Horner SM: WTAP Targets the METTL3 m⁶A-methyltransferase complex to cytoplasmic hepatitis C Virus RNA to regulate infection. *J Virol* 96: e0099722, 2022.
- Yang Z, Wang T, Wu D, Min Z, Tan J and Yu B: RNA N6-methyladenosine reader IGF2BP3 regulates cell cycle and angiogenesis in colon cancer. *J Exp Clin Cancer Res* 39: 203, 2020.
- Chen X, Zhao Q, Zhao YL, Chai GS, Cheng W, Zhao Z, Wang J, Luo GZ and Cao N: Targeted RNA N⁶-Methyladenosine demethylation controls cell fate transition in human pluripotent stem cells. *Adv Sci (Weinh)* 8: e2003902, 2021.
- Dixit D, Prager BC, Gimple RC, Poh HX, Wang Y, Wu Q, Qiu Z, Kidwell RL, Kim LJY, Xie Q, *et al*: The RNA m6A Reader YTHDF2 maintains oncogene expression and is a targetable dependency in glioblastoma stem cells. *Cancer Discov* 11: 480-499, 2021.
- Paris J, Morgan M, Campos J, Spencer GJ, Shmakova A, Ivanova I, Mapperley C, Lawson H, Wotherspoon DA, Sepulveda C, *et al*: Targeting the RNA m⁶A Reader YTHDF2 selectively compromises cancer stem cells in acute myeloid leukemia. *Cell Stem Cell* 25: 137-148.e6, 2019.
- Zhang C, Huang S, Zhuang H, Ruan S, Zhou Z, Huang K, Ji F, Ma Z, Hou B, and He X: YTHDF2 promotes the liver cancer stem cell phenotype and cancer metastasis by regulating OCT4 expression via m6A RNA methylation. *Oncogene* 39: 4507-4518, 2020.
- Jiang W, Zhu P, Huang F, Zhao Z, Zhang T, An X, Liao F, Guo L, Liu Y, Zhou N and Huang X: The RNA methyltransferase METTL3 promotes endothelial progenitor cell angiogenesis in mandibular distraction osteogenesis via the PI3K/AKT Pathway. *Front Cell Dev Biol* 9: 720925, 2021.
- Lin X, Chai G, Wu Y, Li J, Chen F, Liu J, Luo G, Tauler J, Du J, Lin S, *et al*: RNA m⁶A methylation regulates the epithelial mesenchymal transition of cancer cells and translation of Snail. *Nat Commun* 10: 2065, 2019.
- Medina RJ, Barber CL, Sabatier F, Dignat-George F, Melero-Martin JM, Khosrotehrani K, Ohneda O, Randi AM, Chan JKY, Yamaguchi T, *et al*: Endothelial Progenitors: A Consensus Statement on Nomenclature. *Stem Cells Transl Med* 6: 1316-1320, 2017.

25. Avci-Adali M, Nolte A, Simon P, Ziemer G and Wendel HP: Porcine EPCs downregulate stem cell markers and upregulate endothelial maturation markers during in vitro cultivation. *J Tissue Eng Regen Med* 3: 512-520, 2009.
26. Khakoo AY and Finkel T: Endothelial progenitor cells. *Annu Rev Med* 56: 79-101, 2005.
27. Zwaginga JJ and Doevendans P: Stem cell-derived angiogenic/vasculogenic cells: Possible therapies for tissue repair and tissue engineering. *Clin Exp Pharmacol Physiol* 30: 900-908, 2003.
28. Li Z, Qian P, Shao W, Shi H, He XC, Gogol M, Yu Z, Wang Y, Qi M, Zhu Y, *et al*: Suppression of m⁶A reader Ythdf2 promotes hematopoietic stem cell expansion. *Cell Res* 28: 904-917, 2018.
29. Jian D, Wang Y, Jian L, Tang H, Rao L, Chen K, Jia Z, Zhang W, Liu Y, Chen X, *et al*: METTL14 aggravates endothelial inflammation and atherosclerosis by increasing FOXO1 N6-methyladenosine modifications. *Theranostics* 10: 8939-8956, 2020.
30. Zhang M, Yang C, Ruan X, Liu X, Wang D, Liu L, Shao L, Wang P, Dong W and Xue Y: CPEB2 m6A methylation regulates blood-tumor barrier permeability by regulating splicing factor SRSF5 stability. *Commun Biol* 5: 908, 2022.
31. Ping XL, Sun BF, Wang L, Xiao W, Yang X, Wang WJ, Adhikari S, Shi Y, Lv Y, Chen YS, *et al*: Mammalian WTAP is a regulatory subunit of the RNA N6-methyladenosine methyltransferase. *Cell Res* 24: 177-189, 2014.
32. Wang J, Zhang J, Ma Y, Zeng Y, Lu C, Yang F, Jiang N, Zhang X, Wang Y, Xu Y, *et al*: WTAP promotes myocardial ischemia/reperfusion injury by increasing endoplasmic reticulum stress via regulating m⁶A modification of ATF4 mRNA. *Aging (Albany NY)* 13: 11135-11149, 2021.
33. Wei W, Sun J, Zhang H, Xiao X, Huang C, Wang L, Zhong H, Jiang Y, Zhang X and Jiang G: Circ0008399 Interaction with WTAP promotes assembly and activity of the m⁶A methyltransferase complex and promotes cisplatin resistance in bladder cancer. *Cancer Res* 81: 6142-6156, 2021.
34. Wang S, Zhang J, Wu X, Lin X, Liu XM and Zhou J: Differential roles of YTHDF1 and YTHDF3 in embryonic stem cell-derived cardiomyocyte differentiation. *RNA Biol* 18: 1354-1363, 2021.



Copyright © 2023 Wu et al. This work is licensed under a Creative Commons Attribution-NonCommercial-NoDerivatives 4.0 International (CC BY-NC-ND 4.0) License.